Simulation and Optimization of Highly Efficacious Polymer Solar Cell

MOHAMED MOUSA[1], YOUSSEF MOHAMED[1], AHMED MOSTAFA[1], MOSTAFA SALAH[1,*], MOHAMED SENARY[1], MOHAMED HAMOUDA[2]

[1]Electrical Engineering Department
Future University in Egypt
Cairo 11835,
EGYPT

[2]Independent Electricity System Operator (IESO),
Ontario M5H 1T1,
CANADA

Abstract: - This work presents design recommendations to enhance the behavior of polymer solar cells (PSC) through solar cell simulations. The investigated polymer cell comprises a PBDB-T: PZT blend as the active layer, initially structured as ITO/PEDOT-PSS/PBDB-T: PZT/PFN-Br/Ag, achieving a power conversion efficiency (ETA) of approximately 14.91%. Validation of simulation models with experimental data validates the implemented material parameters in the SCAPS-1D simulator. To improve efficiency different materials for the electron transport layer (ETL) are proposed. A suitable ETL should have an energy band offset that matches the absorber material. Various ETLs, such as ZnO, WO_3, ZnOS, and $ZnO_{0.3}S_{0.7}$ are proposed. The front and back contacts' work functions are optimized besides the thicknesses of all layers to improve the efficiency of the proposed PSC. Furthermore, the defect density in the polymer material is studied. Finally, the inverted structure of the simulated PSC is investigated. All previous steps Leeds to increase the ETA of higher than 44%.

Key-Words: - double absorbers, polymers solar cells, PSC, ETA, optimization, PBDB-T:PZT.

Received: May 8, 2024. Revised: October 16, 2024. Accepted: November 19, 2024. Published: December 31, 2024.

1 Introduction

Recently, energy demand has increased because of economic, social, and industrial expansion. However, the present conventional energy supplies will be consumed rapidly over time. It is widely acknowledged. The current energy reserves cannot meet the high demand. Solar cells (SCs), often called photovoltaic (PV) cells, Photovoltaic materials, and equipment turn sunlight into electrical power. A single PV cell is usually modest, delivering around 1 or 2 watts of power, [1].

Photovoltaic (PV) devices provide a long-term answer to the challenges of rising energy demand. Several types of PV technology have been described. The goal is to get higher ETAs while using lower-cost PVs, [2]. Consequently, New thin film solar cells (TFSCs) technologies have been emerging resulting in better efficiencies and reduced prices, [3]. Nowadays, third-generation solar cells, which include dye-sensitized, perovskites, polymers, and bulk heterojunction PVs, are widely researched and quickly evolved, [4].

Why polymer solar cells? Due to their prospective advantages: lightweight, flexibility, high throughput, and large-area manufacturing based on printing and coating processes, [5].

Recent advances in the creation of PSCs have raised power conversion efficiency from 3% to 9% [6], and they have progressively grown every year over the last decade due to considerable research, [7].

In this context, PSCs have sparked significant attention due to their low processing costs, reasonable process flexibility, and lightweight nature, [8]. Furthermore, the thickness of the layers used in PSCs is lowered due to their high material absorption coefficient.

A PSC features a layered architecture formed by an ETL, a polymer absorber material, a hole transport layer (HTL), and contacts. To enhance the ETA of PSCs, various strategies have been pursued,

including modifying the ETL or HTL, optimizing the polymer layer, and improving the interface between the polymer material and the HTL or ETL. For utilizing PSCs in flexible electronics, it is crucial to use low-temperature processed ETLs. Despite advancements, TiO_2 remains the most used ETL in conventional configurations (n-i-p) SCs, benefiting from extensive research over the past two decades, [9].

The present ETAs of PSCs remain less than small molecule acceptor-based organic PVs, owing to the scarcity of polymer acceptors with good behavior accessible for study, [10]. Apart from this, it has been shown that the ETL has a significant impact in controlling PSC, via engineering the band offset at the interfaces. TiO_2 crystals are commonly formed by annealing at temperatures exceeding 450^{o}C, [11]. To bypass the high-temperature annealing procedure, alternative metal oxides that can be treated at low temperatures were investigated as ETL in the proposed PSCs.

In this paper, simulations are employed by SCAPS-1D.

In this paper, the effect of various ETLs on the ETA of PSCs, focusing specifically on zinc oxide (ZnO), tungsten trioxide (WO_3), zinc oxysulfide (ZnOS), and a mixed composition of zinc oxide and sulfur ($ZnO_{0.3}S_{0.7}$) is studied. The ETL electron affinity, the back and front contacts' work functions, the thicknesses of all layers, and the defect density in the active materials are investigated.

This study highlights the nuanced differences in ETL materials and their impact on the efficiency of PSCs, offering insights into optimizing PSC design for improved energy conversion.

2 Modelling and Simulations

SCAPS-1D(3.3.11) is utilized to model and optimize the PSC. SCAPS-1D has been created based on the semiconductors' physics, Poisson's equation, and continuity equations, [12]. Also, the characteristics of individual materials, like the energy gap, affinity, permittivity, mobilities, the density of states, doping, and so on, maybe edited to get the desired structure. Organic semiconductors are frequently employed without intentional doping. The intrinsic charge density (n_i) of an organic film can be derived from its bandgap, spin degeneracy, and the Gaussian dispersion functions that model the HOMO and the LUMO of the molecule, [13]. The PSC includes the following thin layers. The ITO as a right contact, PFN-Br as an ETL, and PEDOT:PSS as an HTL. The active material is PBDB-T:PZT. PBDB-T is the donor while PZT-C1 is the acceptor, [11]. Ag is used as the left contact. The input light is based on air mass 1.5global (AM1.5G). All analyses were conducted at 300 K. The thermal velocity (v_{th}) is assumed to be 10^7 cm/s for all layers. Figure 1 explains the proposed PSC architecture and the energy diagrams of the utilized layers. The input characteristics of the used contacts are recorded in Table 1. The ETL, HTL, and active materials factors are listed in Table 2.

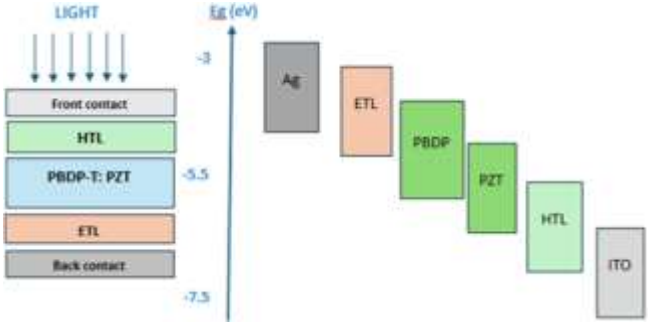

Fig. 1: PSC design and energy diagram.

Table 1. Contacts' characteristics

	Materials	**Work Functions (eV)**	***Sn*(cm/s)**	***Sp*(cm/s)**
Left metal	Ag	4.1	10^5	10^7
Right metal	ITO	4.7	10^7	10^5

Table 2. Layers parameters of the PSC [11], [14]

Parameters	**ETL**	**HTL**	**Polymer**
Thickness (nm)	5	43	100
Bandgap energy E_g (eV)	3	1.3	1.61
Affinities χ (eV)	3.9	3.6	3.69
Relative permittivity ε_r	3.5		3
Conduction, valence band densities N_c, N_v (cm^{-3})	1E+21		
Electron mobilities μ_e (cm^2/VS)	1E-4	8E-4	5.130E-4
Hole mobilities μ_p(cm^2/VS)	1E-6		2.530E-4
Acceptor concentration N_A (cm^{-3})	0	9.2E+18	0

3 Results and Discussions

The performance of the simulated PSC is calibrated with experimental work to validate the used model and materials' parameters, [12]. Figure 2 illustrates the QE and JV curves of the calibration and the experimental work. The main output performance factors are proposed in Table 3 for comparison. The calibration could simulate the experimental work successfully.

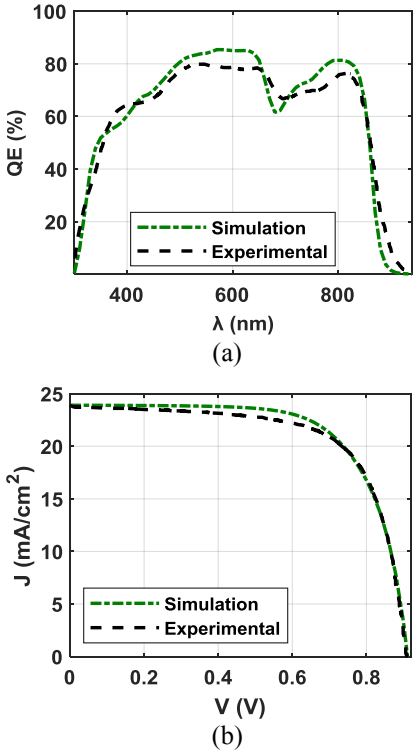

Fig. 2: Comparison between the calibration and the experimental [13] PSCs curves (a) QE and (b) JV

Table 3. Comparison between the calibration and the experimental PSCs performance parameters

	FF [%]	**J_{SC} [mA/cm^2]**	**V_{OC} [V]**	**PCE [%]**
Simulation	68.45	23.9	0.91	14.91
Experimental [11]	68.50	23.9	0.91	14.90

After the calibration, various materials and parameters and materials are investigated to enhance the performance of the PSC.

3.1 ETL Affinity

Electron affinity (EA) is a metric of the energy released when electrons are added to a neutral atom or molecule. It is a significant measure in investigating the electronic properties of materials, particularly in semiconductor physics and photovoltaic applications. In this study, the EA changed between 3.4 eV and 4.5 eV to observe its effect on the ETA of the PSC. Finding an optimal EA of 3.82 eV, which yields a maximum ETA of 15.3%. This relationship highlights the significant influence of EA on the behavior metrics of PVs.

SCs' ETA is impacted by various factors, such as J_{sc}, V_{oc}, and FF. Electron affinity directly affects these parameters in the following ways. For the J_{sc}, electron affinity impacts the band alignment between the acceptor and donor films in the solar cell. Optimal band alignment facilitates efficient charge transfer and reduces recombination losses, thereby increasing the J_{sc}. V_{oc} is influenced by the energy difference between the HOMO and the LUMO.

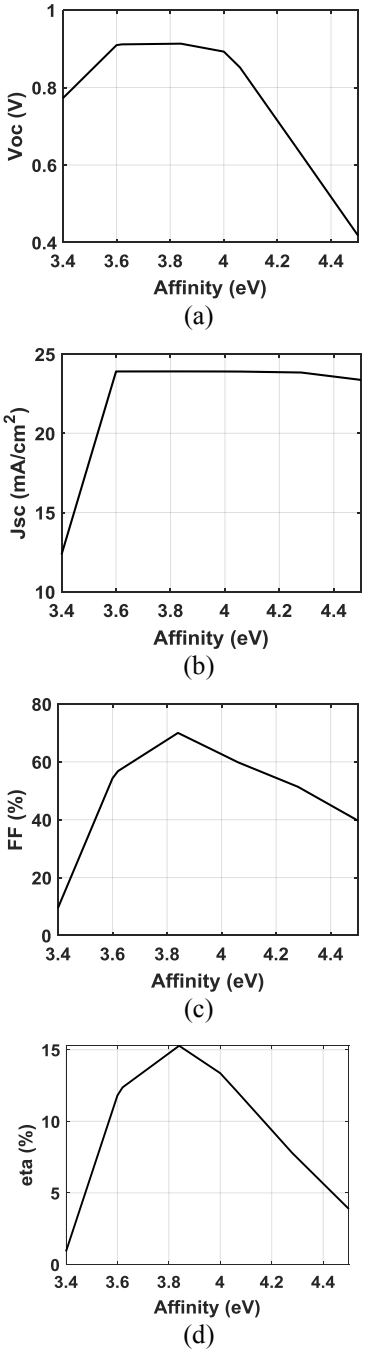

Fig. 3: Output parameters with the ETL's electron affinity

An optimal electron affinity ensures a good energy band alignment, maximizing the V_{oc} by reducing recombination rates and improving charge separation efficiency. FF measures the quality of the SC's current-voltage characteristics. Proper electron affinity leads to optimal charge carrier extraction and minimizes resistive losses, thereby enhancing the FF. Figure 3 describes the influence of the ETL's EA on the main behavior metrics.

3.2 Different Materials for ETL

The structure of the simulated PSC is a p-i-n. The proposed structure is comprised of ITO as a front contact, and Ag as a back contact. PEDOT: PSS as an HTL. The active material is a blend of PBDB-T:PZT. The PBDB-T is a donor while PZT-C1 is an acceptor. PFN-Br as an ETL. IV materials as ETL are proposed instead of the PFN-Br to engineer the conduction band offset (CBO) and enhance the performance. Table 4 lists the factors used in the simulation.

Table 4. ETLs materials parameters, [9]

Parameters	$ZnO_{0.3}S_{0.7}$	WO_3	ZnO	ZnOS
Thickness (nm)	5			
E_g (eV)	3.07	2.6	3.3	2.83
χ (eV)	3.8	3.8	4	3.6
ε_r	9	4.8	9	9
N_c (cm^{-3})	2.2E+21		2.2E+18	
N_v (cm^{-3})	1.8E+18	2.2E+21	1.9E+19	1.8E+19
μ_e (cm^2/VS)	100	30	100	
μ_p (cm^2/VS)	25	20	25	

WO_3 has been proposed as a good candidate ETL in PSCs because of its properties like suitable bandgap energy, fleetly electron transport rate (30 $cm^2\ V^{-1}\ s^{-1}$) compared to PFN-Br (10^{-4} $cm^2\ V^{-1}\ s^{-1}$), and stable in corrosive environments.

ZnO is a good candidate for utilization as an ETL in polymer SCs. It offers a good band offset and high mobility.

Through simulation analysis, $ZnO_{0.3}S_{0.7}$ is determined to exhibit the highest ETA. Table 5 compares the PCEs with various ETLs.

Table 5. Comparison between the PFN-Br-based PSC and various ETLs PSCs PCEs

ETL	PFN-Br	$ZnO_{0.3}S_{0.7}$	WO_3	ZnO	ZnOS
PCE [%]	14.91	16.2	15.28	15.12	14.17

3.3 Effect of Contacts' Work Functions

In the context of photovoltaic devices, the creation of Schottky barrier contacts is a critical factor influencing device performance. This occurs when the work function of the metal (ϕ_m) is less than the addition of the energy gap (E_g), the EA of the active layer (δ_{Abs}), and the energy difference in the valence (or conduction) band between the bulk and the edge (ϕ_d).

The formation of the Schottky barrier (ϕ_s) at the contact can be expressed as $\phi_s = \phi_m - E_v$, where E_v represents the valence band energy. Reducing the Schottky barrier height is desirable as it leads to a more ohmic-like contact, enhancing charge carrier transport and overall device efficiency.

To optimize the Schottky barrier height for a given absorber material, selecting a back contact metal with a work function of ($\delta_{Abs} + \phi_d + E_g$) is effective. Alternatively, using a metal with a high work function is beneficial when dealing with a p^+ active material.

In the proposed simulations of solar cells, the work functions of the metals are studied to observe their impact on the device performance. By carefully tuning the work function, the Schottky barrier height is reduced, thereby enhancing the efficiency and performance of the solar cells.

a) Impact of back contact work function: Figure 4 shows the effect of the back contact work f (left contact) on the behavior metrics of the cell when the ETL is $ZnO_{0.3}S_{0.7}$. The best performance is achieved when the work function of back contact is 3.7 eV with the highest ETA of 17.27% which improved by 1.07%, FF of 78.98%, V_{oc} of 0.913 V, and J_{sc} of 23.93 mA/cm^2.

b) Impact of Front Contact Work Function: Figure 5 illustrates the influence of the front contact work function (right contact) on the performance parameters of the PSC when the back contact work function is 3.7 eV. The best performance is achieved when the front contact work function is 5.2 eV with ETA of 19.52% which improved by 2.25 %, FF of 74.43%, V_{oc} of 1.09 V, and J_{sc} of 24.02 mA/cm^2.

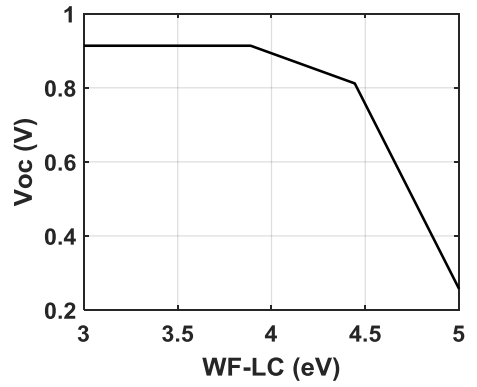

(a)

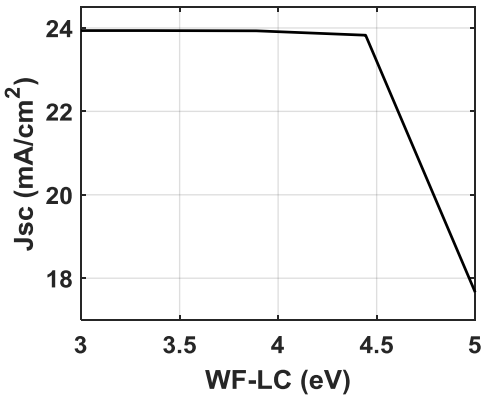

(b)

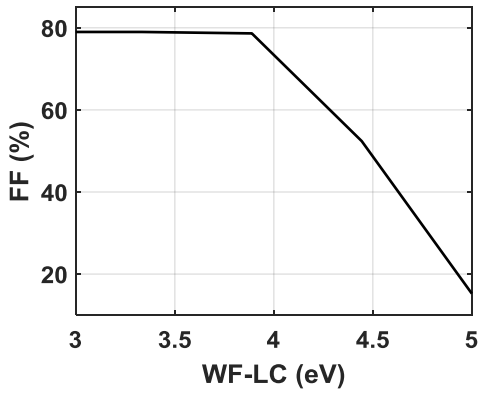

(c)

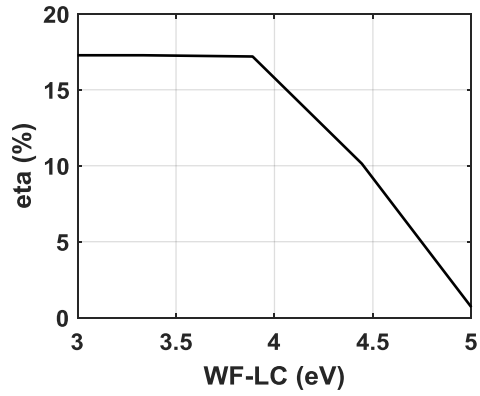

(d)

Fig. 4: Output parameters with the back metal work function

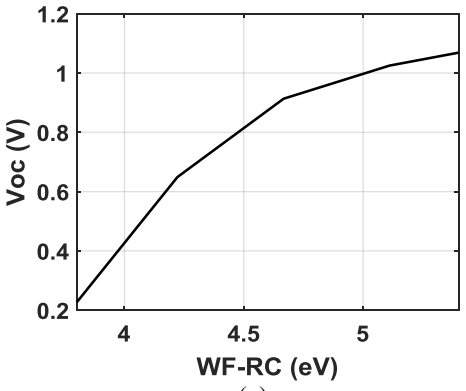

(a)

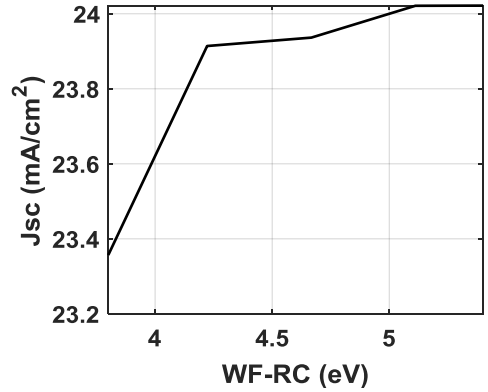

(b)

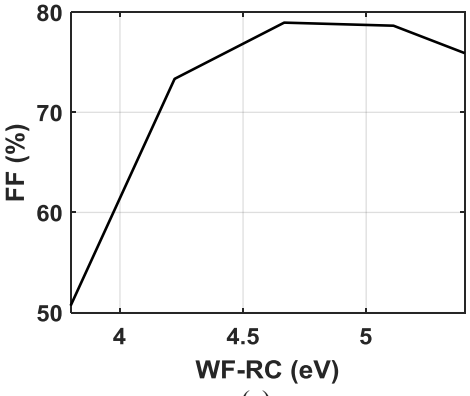

(c)

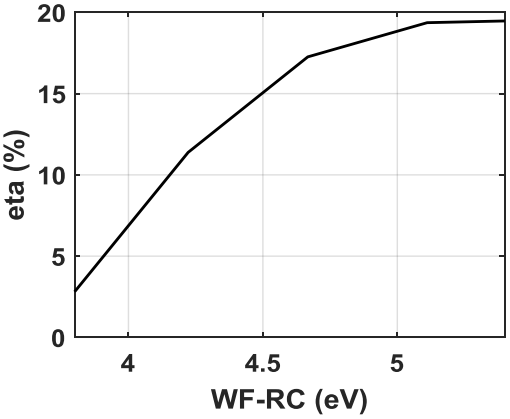

(d)

Fig. 5: Behaviour metrics with the front contact work function

4 Impact of the HTL Thickness

Figure 6 illustrates the impact of the thickness of the HTL on the behavior metrics of the PSC. The best behavior is achieved when the thickness of the HTL is 10 µm with an ETA of 31.58% which increased by 12%, FF of 75.3%, V_{oc} of 1.1 V, and J_{sc} of 38.04 mA/cm^2. At this thickness, the HTL acts as an absorber besides the hole transportation. Consequently, in this case, the cell has double absorbers which explain the performance enhancement.

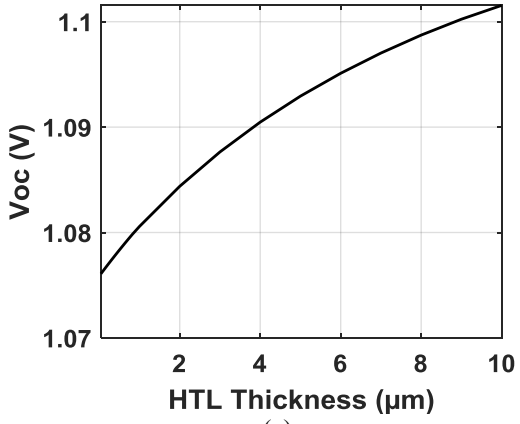

(a)

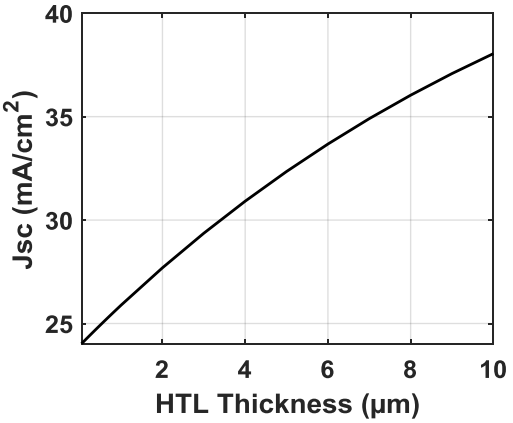

(b)

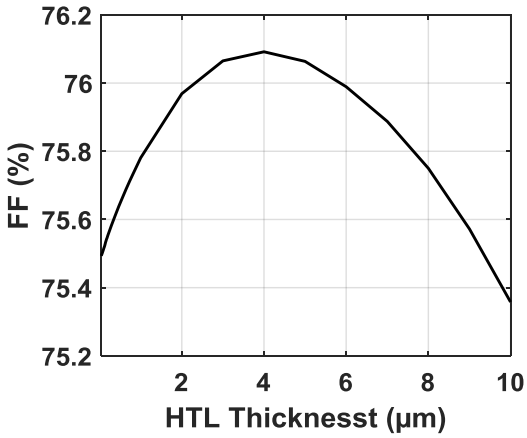

(c)

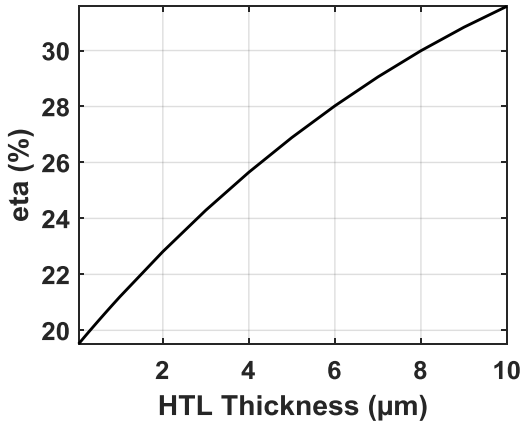

(d)

Fig. 6: Output metrics with the HTL thickness

5 Impact of the Absorber Material Thickness

Figure 7 illustrates the influence of the thickness of absorber material on the behavior metrics when the thickness of the HTL is 10 µm. The optimum behavior is achieved when the thickness of the absorber layer is 74 nm with the highest ETA of 31.67%, FF of 77.72%, V_{oc} of 1.1 V, and J_{sc} of 36.97 mA/cm^2.

6 Impact of the ETL Thickness

Figure 8 illustrates the effect of the thickness of the ETL on the behavior metrics of the PSC when the thickness of the active film is 74 nm and the thickness of HTL is 10 µm. The optimum behavior is achieved when the thickness of the ETL is 1 nm with an ETA of 31.97% which is improved by 0.3%, FF of 78.51%, V_{oc} of 1.102 V, and J_{sc} of 36.938 mA/cm^2.

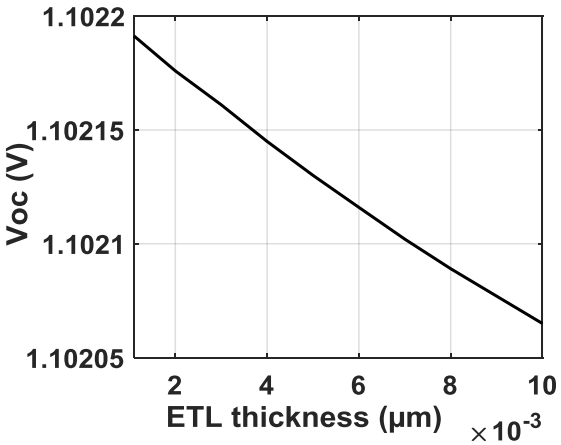

(a)

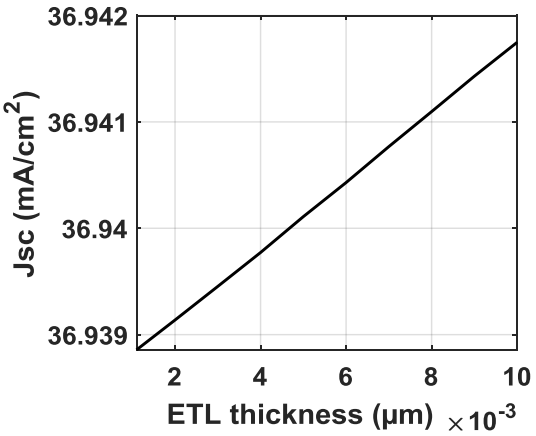

(b)

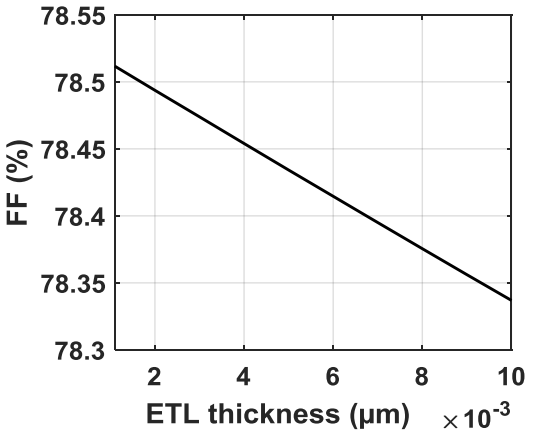

(c)

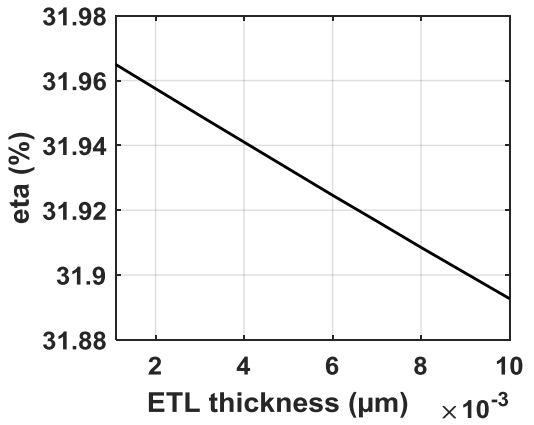

(d)

Fig. 8: Output parameters with the ETL thickness

7 Impact of the Polymer Bulk Defect Density

Figure 9 illustrates the total defect density on the behavior parameters of the PSC. The best behavior is achieved when the total defect density is 1E9 cm^{-3} with ETA of 33.04% which improved by 1.07 %, FF of 80.81%, V_{oc} of 1.106 V, and J_{sc} of 36.94 mA/cm^2.

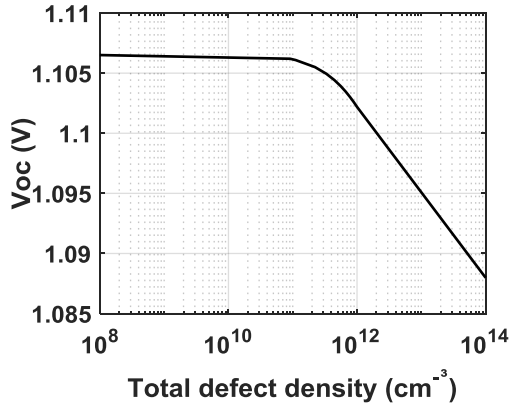

(a)

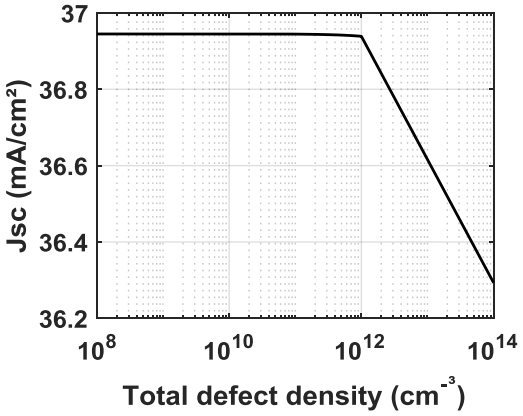

(b)

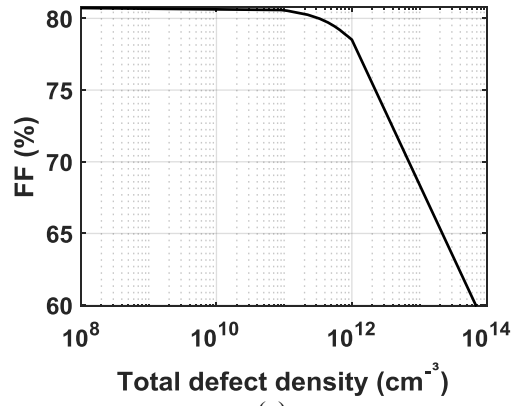

(c)

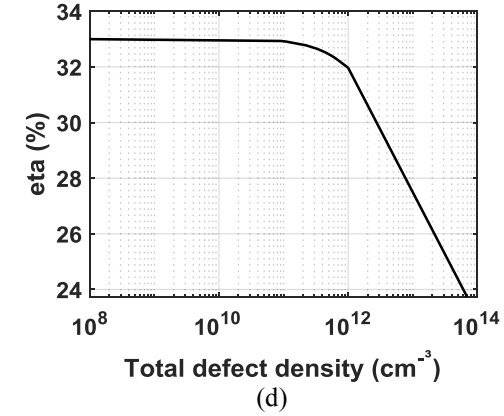

(d)

Fig. 9: Output parameters with the N_t of the absorber

8 n-i-p Structure and State of the Comparison

The calibrated PSC started with ETA of 14.91%, FF of 68.45%, V_{oc} of 0.9115 V, and J_{sc} of 23.9 mA/cm^2. After the optimization and ETL material selection, an encouraging result is obtained. The highest ETA of the optimized PSC is 33.04%, FF of 80.81%, V_{oc} of 1.106 V, and J_{sc} of 36.94 mA/cm^2. When the structure is inverted, which means the structure is n-i-p instead of p-i-n, an encouraging result is achieved. The highest ETA of the optimized inverted PSC is 44.48%, FF of 81.21%, V_{oc} of 1.119 V, and J_{sc} of 48.91 mA/cm^2. Table 6 compares the achieved results in this paper with the literature.

Photovoltaics is the most significant renewable energy source, [16], [17]. So, this work opens the potential to enhance PSCs.

Table 6. PCEs comparison between recent PSCs.

Active Blend	ETL	ETA (%)	Notes	Ref.
PBDB-T:PZT-γ	PFN-Br	15.80	Exp.	[10]
PBDB-T:PZT-C1	PFN	14.90	Exp.	[11]
PBDB-T:PN-Se	PDINN	16.16	Exp.	[13]
PBDB-T:PZT	PFN-Br	14.91	Sim.	[5]
PBDB-T:PZT	PFN-Br	22.85	Double HTL	[5]
PBDB-T:PZT	PFN-Br	22.67	Inverted structure	[15]
PBDB-T:PZT	$ZnO_{0.3}S_{0.7}$	33.04	Sim.	This work
PBDB-T:PZT	$ZnO_{0.3}S_{0.7}$	44.48	Inverted structure	This work

9 Conclusion and Future Work

In this paper, a PSC has been proposed and optimized utilizing SCAPS-1D. The initial ETA was 14.91%. The behavior of the proposed PSC has been studied to evaluate the significant impact of the barrier between the ETL and the back contact, as well as between the ETL and the absorber. The performance of various ETLs has been compared. The outputs show that $ZnO_{0.3}S_{0.7}$ is the best candidate for the ETL. After optimization of the work functions of the front and back contacts an ETA of 19.52% is achieved. Optimization of all layer thicknesses resulted in an ETA of 31.97%. The bulk defect density in the active material has a great impact on the behavior of the PSCs. When the total defect density is 1E9 cm^{-3} an ETA of 33.04% was achieved. Finally, the inverted structure of the optimized cell was 44.48%.

The proposed work could open the potential to improve PSCs.

In future work, the optimized cell will be experimentally implemented to validate the achieved results.

References:

[1] M.C. Putnam, S.W. Boettcher, M.D. Kelzenberg, D.B. Turner-Evans, J.M. Spurgeon, E.L. Warren, R.M. Briggs, N.S. Lewis, H.A. Atwater, Si microwire-array solar cells, Energy Environ Sci 3 (2010) 1037–1041. https://doi.org/10.1039/C0EE00014K.

[2] M.S. Salem, A.J. Alzahrani, R.A. Ramadan, A. Alanazi, A. Shaker, M. Abouelatta, C. Gontrand, M. Elbanna, A. Zekry, Physically Based Analytical Model of Heavily Doped Silicon Wafers Based Proposed Solar Cell Microstructure, IEEE Access 8 (2020) 138898–138906. https://doi.org/10.1109/ACCESS.2020.3012657.

[3] M. Salem, A. Zekry, M. Abouelatta, M.T. Alshammari, A. Alanazi, K.A. Al-Dhlan, A. Shaker, Influence of base doping level on the npn microstructure solar cell performance: A TCAD study, Opt Mater (Amst) 121 (2021) 111501. https://doi.org/10.1016/J.OPTMAT.2021.111501.

[4] G. Kim, G. Kim, J.W. Lim, J.W. Lim, J. Kim, J. Kim, S.J. Yun, S.J. Yun, M.A. Park, Transparent Thin-Film Silicon Solar Cells for Indoor Light Harvesting with Conversion Efficiencies of 36% without Photodegradation, ACS Appl Mater Interfaces 12 (2020) 27122–27130. https://doi.org/10.1021/acsami.0c04517.

[5] M. S. Salem, A. Shaker, and M. M. Salah, "Device Modeling of Efficient PBDB-T:PZT-Based All-Polymer Solar Cell: Role of Band Alignment," *Polymers (Basel)*, vol. 15, no. 4, 2023, doi: 10.3390/polym15040869.

[6] M.A. Green, E.D. Dunlop, M. Yoshita, N. Kopidakis, K. Bothe, G. Siefer, X. Hao, Solar cell efficiency tables (Version 63), Progress in Photovoltaics: Research and Applications 32

(2024) 3–13. https://doi.org/10.1002/PIP.3750.M.

[7] Okil, M. S. Salem, T. M. Abdolkader, and A. Shaker, "From Crystalline to Low-cost Silicon-based Solar Cells: a Review," *Silicon 2021 14:5*, vol. 14, no. 5, pp. 1895–1911, Mar. 2021, doi: 10.1007/S12633-021-01032-4.

[8] P. Gnida, M. F. Amin, A. K. Pajak, and B. Jarzabek, "Polymers in High-Efficiency Solar Cells: The Latest Reports," *Polymers 2022, Vol. 14, Page 1946*, vol. 14, no. 10, p. 1946, May 2022, doi: 10.3390/POLYM14101946.

[9] Y. Xiao, C. Wang, K.K. Kondamareddy, P. Liu, F. Qi, H. Zhang, S. Guo, X.Z. Zhao, Enhancing the performance of hole-conductor free carbon-based perovskite solar cells through rutile-phase passivation of anatase TiO2 scaffold, J Power Sources 422 (2019) 138–144. https://doi.org/10.1016/J.JPOWSOUR.2019.03.039.

[10] H. Fu, Y. Li, J. Yu, Z. Wu, Q. Fan, F. Lin, H.Y. Woo, F. Gao, Z. Zhu, A.K.Y. Jen, High efficiency (15.8%) all-polymer solar cells enabled by a regioregular narrow bandgap polymer acceptor, J Am Chem Soc 143 (2021) 2665–2670. https://doi.org/10.1021/JACS.0C12527/SUPPL_FILE/JA0C12527_SI_001.PDF.

[11] H. Fu, Y. Li, Z. Wu, F. R. Lin, H. Y. Woo, and A. K. Y. Jen, "Side-Chain Substituents on Benzotriazole-Based Polymer Acceptors Affecting the Performance of All-Polymer Solar Cells," *Macromol Rapid Commun*, vol. 43, no. 16, p. 2200062, Aug. 2022, doi: 10.1002/MARC.202200062.

[12] M. Burgelman, K. Decock, A. Niemegeers, J. Verschraegen, and S. Degrave, "SCAPS manual".

[13] J. Du, K. Hu, J. Zhang, L. Meng, J. Yue, I. Angunawela, H. Yan, S. Qin, X. Kong, Z. Zhang, B. Guan, H. Ade, Y. Li, Polymerized small molecular acceptor based all-polymer solar cells with an efficiency of 16.16% via tuning polymer blend morphology by molecular design, Nature Communications 2021 12:1 12 (2021) 1–10. https://doi.org/10.1038/s41467-021-25638-9.

[14] A. N. M. Alahmadi, "Design of an Efficient PTB7:PC70BM-Based Polymer Solar Cell for 8% Efficiency," *Polymers 2022, Vol. 14, Page 889*, vol. 14, no. 5, p. 889, Feb. 2022, doi: 10.3390/POLYM14050889.

[15] T. I. Al-Muhimeed, S. Alahmari, M. Ahsan, and M. M. Salah, "An Investigation of the Inverted Structure of a PBDB:T/PZT:C1-Based Polymer Solar Cell," *Polymers (Basel)*, vol. 15, no. 24, 2023, doi: 10.3390/polym15244623.

[16] M. A. M. Shaheen, H. M. Hasanien, R. A. Turky, M. Ćalasan, A. F. Zobaa, and S. H. E. A. Aleem, "Opf of modern power systems comprising renewable energy sources using improved chgs optimization algorithm," *Energies (Basel)*, vol. 14, no. 21, 2021, doi: 10.3390/en14216962.

[17] S. Fouda, M.S. Salem, A. Saeed, A. Shaker, M. Abouelatta, Thirteen-level modified packed u-cell multilevel inverter for renewable-energy applications, 2020 2nd International Conference on Smart Power and Internet Energy Systems, SPIES 2020 (2020) 431–435. https://doi.org/10.1109/SPIES48661.2020.9243059.

Contribution of Individual Authors to the Creation of a Scientific Article (Ghostwriting Policy)

The authors equally contributed in the present research, at all stages from the formulation of the problem to the final findings and solution.

Sources of Funding for Research Presented in a Scientific Article or Scientific Article Itself

No funding was received for conducting this study.

Conflict of Interest

The authors have no conflicts of interest to declare.